Growth and Characterization of Photoactive and Electroactive Zirconium Bisphosphonate Multilayer Films

Jonathan L. Snover,† Houston Byrd,‡ Elena P. Suponeva, Edward Vicenzi,§ and Mark E. Thompson*

Department of Chemistry, University of Southern California, Los Angeles, California 90089-0744

Received January 30, 1996. Revised Manuscript Received April 25, 1996⊗

Zirconium alkylbisphosphonates are prepared by treating a derivatized substrate alternately with solutions of Zr^{4+} and a bisphosphonic acid. We report here the preparation of electroactive and photoactive metal phosphonate thin films, containing neutral and cationic organic groups. Electronic spectroscopy, ellipsometry, atomic force microscopy, and electron probe microanalysis were used to characterize the structure and composition of these thin films. An *N*,*N*′-dialkylphenylenediamine bisphosphonate (1,4-bis(4-phosphonobutylamino)-benzene) gives uniform lamellar thin films, with low root-mean-square roughness. The stoichiometry of this film is low in Zr relative to other zirconium bisphosphonate films [i.e., $Zr_{0.75}$(bisphosphonate)]. Bisphosphonic acids with cationic organic groups (e.g., $H_2O_3PCH_2$-CH_2−(4,4′-bipyridinium)−$CH_2CH_2PO_3H_2$) do not follow the typical layered growth motif but instead form crystallites on the substrate surface. Lamellar growth in films prepared with neutral bisphosphonic acids can be perturbed by adding ammonium ions to the bisphosphonic acid growth solutions, leading to the growth of large crystallites. Electrochemical studies were carried out on crystallite films of viologen bisphosphonate based materials, grown on both gold foil and Sn[Sb]O_x-coated glass substrates. The estimated reduction potential for viologen in these films (−0.83 V) is independent of film thickness but shows kinetic limitations that are directly related to film thickness. The $E°$ of the viologen moiety in ZrPV(X) films is 150 mV more negative than that of dimethylviologen in solution or in other thin films.

Introduction

Metal phosphonate multilayer film assemblies have attracted attention because of their ease of preparation and physical stability.[1−6] Thin-film growth involves sequential adsorption of organobisphosphonic acids and metal ions on a derivatized substrate, leading to layer-by-layer growth. This sequential growth technique provides ready control of film thickness and composition on a molecular level. The growth of these films is generally thought to proceed as shown in Figure 1. Researchers have utilized metal phosphonate thin films (first reported by Mallouk, et al.[7]) to study systems where interlayer distance and orientation of the organic components are crucial, such as electron transfer,[8] nonlinear optics,[9,10] photocatalysis,[11] and molecular recognition.[12] Several thorough reviews on metal phosphonate films and solids have recently been published.[2,12−15]

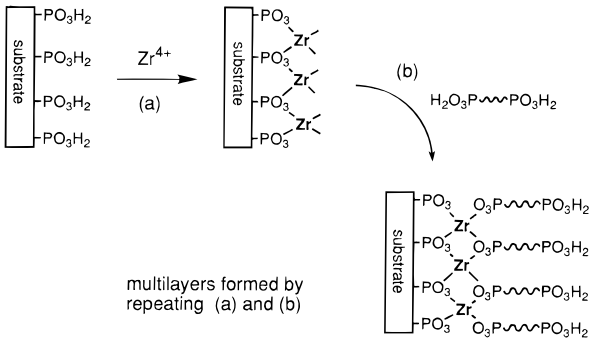

Figure 1. Steps in the growth of multilayer films.

The majority of the studies involving metal phosphonate films have been carried out with alkyl bisphosphonates. The lamellar nature of long-chain alkyl bispho-

* To whom correspondence should be addressed.
† Current address: Department of Chemistry, North Carolina State University, Raleigh, NC 27695.
‡ Permanent address: Department of Chemistry, Montevallo University, Montevallo, AL 35115.
§ Princeton Materials Institute, Princeton University, Princeton, NJ 08544.
⊗ Abstract published in *Advance ACS Abstracts,* June 1, 1996.

(1) Alberti, G.; Constantino, U.; Alluli, S.; Tomassini, N. *Inorg. Nucl. Chem.* **1978**, *40*, 1113−1117.
(2) Alberti, G.; Constantino, U.; Alberti, G.; Constantino, U., Ed.; Oxford University Press: Oxford, 1991, pp Chapter 5.
(3) DiGiacomo, P. M.; Dines, M. B. *Polyhedron* **1982**, *1*, 61−68.
(4) Dines, M. B.; DiGiacomo, P. M. *Inorg. Chem.* **1981**, *20*, 92−97.
(5) Dines, M. B.; Griffith, P. C. *Inorg. Chem.* **1983**, *22*, 567−569.
(6) Troup, J. M.; Clearfield, A. *Inorg. Chem.* **1977**, *16*, 3311−3314.
(7) Lee, H.; Kepley, L. J.; Hong, H.-G.; Mallouk, T. E. *J. Am. Chem. Soc.* **1988**, *110*, 618−620.
(8) Ungashe, S. B.; Wilson, W. L.; Katz, H. E.; Scheller, G. R.; Putivinski, T. M. *J. Am. Chem. Soc.* **1992**, *114*, 8717−8719.
(9) Katz, H. E.; Scheller, G.; Putvinski, T. M.; Schilling, M. L.; Wilson, W. L.; Chidsey, C. E. D. *Science* **1991**, *254*, 1485−1487.
(10) Putvinski, T. M.; Schilling, M. L.; Katz, H. E.; Chidsey, C. E. D.; Mujsce, A. M.; Emerson, A. B. *Langmuir* **1990**, *6*, 1567−1571.
(11) Snover, J. L.; Thompson, M. E. *J. Am. Chem. Soc.* **1994**, *116*, 765−766.
(12) Cao, G.; Hong, H.-G.; Mallouk, T. E. *Acc. Chem. Res.* **1992**, *25*, 420−427.
(13) Katz, H. E. *Chem. Mater.* **1994**, *6*, 2227−2232.
(14) Clearfield, A. *Comments Inorg. Chem.* **1990**, *10*, 89.
(15) Thompson, M. E. *Chem. Mater.* **1994**, *6*, 1168−1175.

S0897-4756(96)00058-0 CCC: $12.00

sphonate films have been determined in several cases by researchers using ellipsometry[7,10,16−18] and a variety of X-ray techniques.[18−22] Films composed of shorter alkyl chains are not as well ordered, presumably because they lack the strong van der Waals interactions associated with the long chains.[23,24] The body of data which has accumulated on aliphatic bisphosphonate films suggests that they are relatively well ordered with a structure related to the microcrystalline bulk solids. In these materials the axes of the aliphatic chains make roughly a 30° angle to inorganic lamellae.[7,10,16−22] This structure is consistent with a structural model for the thin films in which inorganic layers are formed [i.e., $Zr(O_3P-)_2$], with the organic groups lying in the interlayer space. The inorganic lamellae in this model have a structure similar to that of α-$Zr(O_3POH)_2 \cdot H_2O$ (α-ZrP). Although these films give good surface coverage and are fairly dense, it has been shown that they often contain defects.[25] These defects are attributed to a mismatch between the inorganic (i.e., $Zr(O_3P-)_2$) and organic networks. We have recently carried out a study in which we examined a growing zirconium hexadecylbisphosphonate film by AFM.[26] This material grows as islands in the early stages of growth, leading to a very imperfect film, but ultimately gives a uniform coating on the silicon substrate after 3−4 h of treatment. Less information has been obtained on the structures of films that contain organic components with useful optical or electronic properties. Although data suggest that these sorts of films are dense and well aligned,[9,10] they have not been shown to grow with the degree of uniformity observed in the films grown with aliphatic bisphosphonates. Optimizing the structures of the bisphosphonic acids in the film, so that superior films can be grown, is necessary for the benefits of this multilayer technique to be realized.

One of the goals of our research is to incorporate photoactive species into multilayer assemblies, in order to prepare thin films which undergo efficient photoinduced charge separation and catalysis. In this paper we describe the characterization of several metal phosphonate films using ellipsometry, UV/vis spectroscopy, atomic force microscopy, and electron probe microanalysis (EPMA). Comparing these data to those of the solid analogues can provide insight into the structure and composition of these films. Alkyl bisphosphonic acids with phenylenediamine groups in the alkyl chain (i.e., $H_2O_3P-(CH_2)_4-NHC_6H_4NH-(CH_2)_4-PO_3H_2$) give uniform lamellar thin films, as shown by ellipsometry and atomic force microscopy (AFM). In contrast, metal phosphonate films formed from alkyl bisphosphonic acids with charged organic components (i.e., $H_2O_3P-(CH_2)_2-4,4'-\text{bipyridinium}-(CH_2)_2-PO_3H_2$) consist of crystallites, which form in islands on the substrate surface. Furthermore, films which normally grow in a lamellar manner can be influenced to grow in a crystallite fashion by adding small amounts of ammonium salts to the phosphonic acid solutions. Understanding the structure and composition of these films is crucial for future design of more complex composite assemblies. To study macroscopic electron transfer in these films, electrochemical studies were carried out on films of viologen bisphosphonate based materials, grown on both gold foil and $Sn[Sb]O_x$-coated glass substrates. The estimated reduction potential for viologen in these films (−0.83 V) is independent of film thickness but shows kinetic limitations that are directly related to film thickness.

Scheme 1

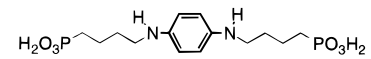

BAB

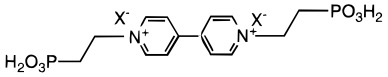

PV(X)

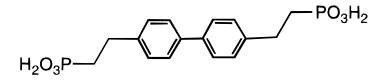

EPB

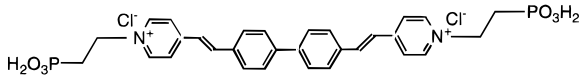

VPB

Results and Discussion

Characterization of Metal Phosphonate Thin Films. The growth and structure of multilayer films of zirconium 1,4-bis(4-phosphonobutylamino)benzene (ZrBAB, see Scheme 1) have been studied in detail. This diamine was designed to be incorporated into multilayers as an electron donor. Figure 2 shows the increase in absorbance (at 270 nm) and ellipsometric thickness as a function of the number of layers. The linear increase in absorbance indicates that the same amount of material is being deposited in each treatment but does not verify uniform layer growth. Ellipsometric data are a better indication of uniformity and complete coverage since it measures an average thickness; however, it can also be misleading since the measurement is an average over a macroscopic area. If the layers are relatively tightly packed and uniform, the measured layer thickness should be close to the value seen in the bulk solid, and the deviation in the measurements at various points on the substrate should be small. The slope of the line in Figure 2 gives a layer thickness of 22 Å/layer, which

(16) Katz, H. E.; Schilling, M. L.; Chidsey, C. E. D.; Putvinski, T. M.; Hutton, R. S. *Chem. Mater.* **1991**, *3*, 699−703.
(17) Lee, H.; Kepley, L. J.; Hong, H.-G.; Akhter, S.; Mallouk, T. E. *J. Phys. Chem.* **1988**, *92*, 2597−2601.
(18) Zeppenfeld, A. C.; Fiddler, S. L.; Ham, W. K.; Klopfenstein, B. J.; Page, C. J. *J. Am. Chem. Soc.* **1994**, *116*, 9158−9165.
(19) Akhter, S.; Lee, H.; Hong, H.-G.; Mallouk, T. E.; White, J. M. *J. Vac. Sci. Technol., A* **1989**, *7*, 1608−1613.
(20) Byrd, H.; Pike, J. K.; Talham, D. R. *Chem. Mater.* **1993**, *5*, 709−715.
(21) Hong, H.-G.; Sackett, D. D.; Mallouk, T. E. *Chem. Mater.* **1991**, *3*, 521−527.
(22) Umemura, Y.; Tanaka, K.; Yamagishi, A. *J. Chem. Soc., Chem. Commun.* **1992**, 67−68.
(23) O'Brien, J. T.; Zeppenfeld, A. C.; Richmond, G. L.; Page, C. J. *Langmuir* **1994**, *10*, 4657−4663.
(24) Porter, M. D.; Bright, T. B.; Allara, D. A.; Chidsey, C. E. *J. Am. Chem. Soc.* **1987**, *109*, 3559.
(25) Schilling, M. L.; Katz, H. E.; Stein, S. M.; Shane, S. F.; Wilson, W. L.; Buratto, S.; Ungashe, S. B.; Taylor, G. N.; Putvinski, T. M.; Chidsey, C. E. D. *Langmuir* **1993**, *9*, 2156−2160.
(26) Byrd, H.; Snover, J. L.; Thompson, M. E. *Langmuir* **1995**, *11*, 4449−4453.

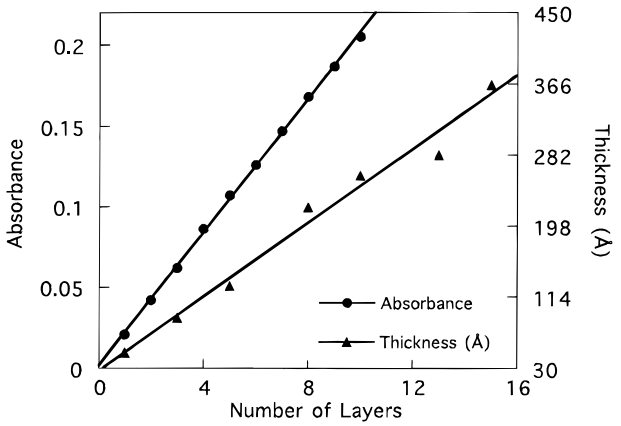

Figure 2. Thickness and absorbance as a function of layers for a ZrPAPD film. Absorption was obtained on SiO_2 substrates at 270 nm. Elipsometric thickness was obtained on Si assuming a film refractive index of 1.45. Best fit of the data gives a slope of 22 Å.

is consistent with a planar inorganic layer which has the phosphonate bound butyl chain axes tilted at 30° relative to the substrate normal. This chain orientation is the same observed for simple metal α,ω-alkylbisphosphonate compounds.[23] Ellipsometric thicknesses measured at various points on the substrate surface show very little deviation (±5 Å), as expected for a lamellar thin film.

While both UV/vis spectra and ellipsometric measurements suggest that the ZrBAB films grow uniformly, they are not conclusive. Atomic force microscopy (AFM) is a useful technique for studying film uniformity and growth on a microscopic level.[26] Studying the surface features of an assembling film can be useful in examining the mode of layer growth. Film roughness is a good value to use in comparing the uniformity of films. Polished silicon has a root-mean-square (rms) roughness of 1−2 Å. A uniform monolayer of a long-chain alkyl bisphosphonate produces a roughness of 2−3 Å. Films that are uniform and fully assembled should have smooth surfaces by AFM, and those that are incomplete or defected should have rough surfaces. A 10-layer film of ZrBAB on Si produces a surface with a roughness of 17 Å, which is less than the monolayer thickness (Figure 3). The surface of this film appears very smooth with an occasional large feature, which we ascribe to dust particles or other foreign objects (these films are grown in a synthetic lab and not a clean room environment). This film is 220 Å thick (by ellipsometry), so a 17 Å deviation is consistent with a uniform and tightly packed lamellar film.

The composition of films of ZrBAB were examined by EPMA. It is important to consider matrix effects in evaluating the validity of elemental ratios determined from EPMA data on thin film samples. Matrix corrections applied to conventional electron probe data are carried out under the assumption that the activation microvolume is chemically homogeneous. In this study metal phosphonate films deposited on Si/SiO_2 typically have a film thickness of 200−300 Å, as measured by ellipsometry. Using a typical electron beam energy of 15 kV (often chosen because one can easily excite X-ray lines across the periodic table) the ionization depth will clearly exceed the film thickness (>2.5 μm). The substrate becomes a large portion of the activation volume owing to electron scattering as incident energies are diminished, which ultimately leads to lateral beam spreading. Such "oversampling" will lead to inaccurate compositions as a result of (1) characteristic radiation of the substrate causing potential X-ray fluorescence of lower energy lines in the film, (2) a change in the backscatter coefficient, which must be known to estimate the percentage of elastically scattered electrons (or those not responsible for X-ray generation), and (3) continuum radiation produced in the substrate that will affect the X-ray yield of the film. We have evaluated these uncertainties by performing a series of analyses at electron beam energies of 5, 10, and 15 kV as well as by applying a set of matrix corrections which account for the nonhomogeneity of a film/substrate geometry using the program STRATA.[27] Data collected under a variety of conditions can be fitted to accurate analytical expressions of the intensity depth distribution often referred to as the $\Phi(\rho,Z)$ function.[28] The amounts of zirconium per 2 phosphorus atoms ($\pm 1\ \sigma$ of the population) at 5, 10, and 15 kV are 0.75 ± 0.14, 0.76 ± 0.11, and 0.65 ± 0.13, respectively, while the ratio computed by STRATA is 0.73. One may conclude that cationic ratios of metal phosphonate films deposited on substrates of moderately low Z (i.e., Si) determined at one experimental condition are in excellent agreement with the results of the sophisticated matrix correction scheme employed by STRATA. It is important to point out that the similarity in results from these two methods (i.e., variable accelerating voltage and STRATA) will not necessarily be found in films of different composition, and almost certainly not with higher Z substrate materials. Marinenko compared thin-film microchemistry determined by variable-voltage EPMA and Rutherford backscattering (RBS).[29] RBS is widely regarded as a technique that can accurately measure thin-film compositions. The author found that EPMA gave very similar results (within the uncertainty of each method).

At first glance the ratio of Zr to P for ZrBAB looks to be low in Zr, relative to a conventional zirconium bisphosphonate (expect Zr:P = 1:2). It is possible to rationalize the observed stoichiometry, however, by recognizing that the phenylenediamine group will carry positive charge under the experimental growth conditions. The pK_{a_1} and pK_{a_2} values for *N*,*N*′-di-*n*-heptyl-*p*-phenylenediamine are 6.8 and 2.65, respectively.[30] BAB should have a very similar pK_a values, so that the phenylenediamime groups of BAB should be singly protonated under our growth conditions (the pH of the BAB solution is 3). In addition to protonation, aerobic oxidation can give a radical cation (Wurtz salt) of phenylenediamine.[31] While we see evidence for the Wurtz salt in the electronic spectra of aged BAB solutions, the spectra of ZrBAB films show insignificant levels of the Wurtz salt. Protonation of the phenylene diamine groups of BAB will give the molecule an overall charge of −3 (−4 for the phosphonates and +1 for the

(27) STRATA is a registered trademark of SAMX Co., rue Galilee, 78280 Guyancourt, France; STRATA is a registered trademark of SAMX Co., rue Galilee, 78280 Guyancourt, France, Ed.

(28) Pouchou, J. L.; Pinchoir, F. *Scanning* **1990**, *12*, 212−214.

(29) Marinenko, R. B. *Proceedings of the 13th Internation Congress on Electron Microscopy, Paris, July 17−22*; Marinenko, R. B., Ed.; Les Editions de Physique: France, 1994; Vol. 1, Interdisciplinary Developments and Tools, pp 705−706.

(30) Albert, F. M.; Giurginca, M.; Meghea, A.; Ivan, G. *Rev. Roum. Chem.* **1980**, *25*, 1543−1548.

(31) Michaelis, L.; Schubert, M. D.; Granick, S. *J. Am. Chem. Soc.* **1939**, *61*, 1981−1992.

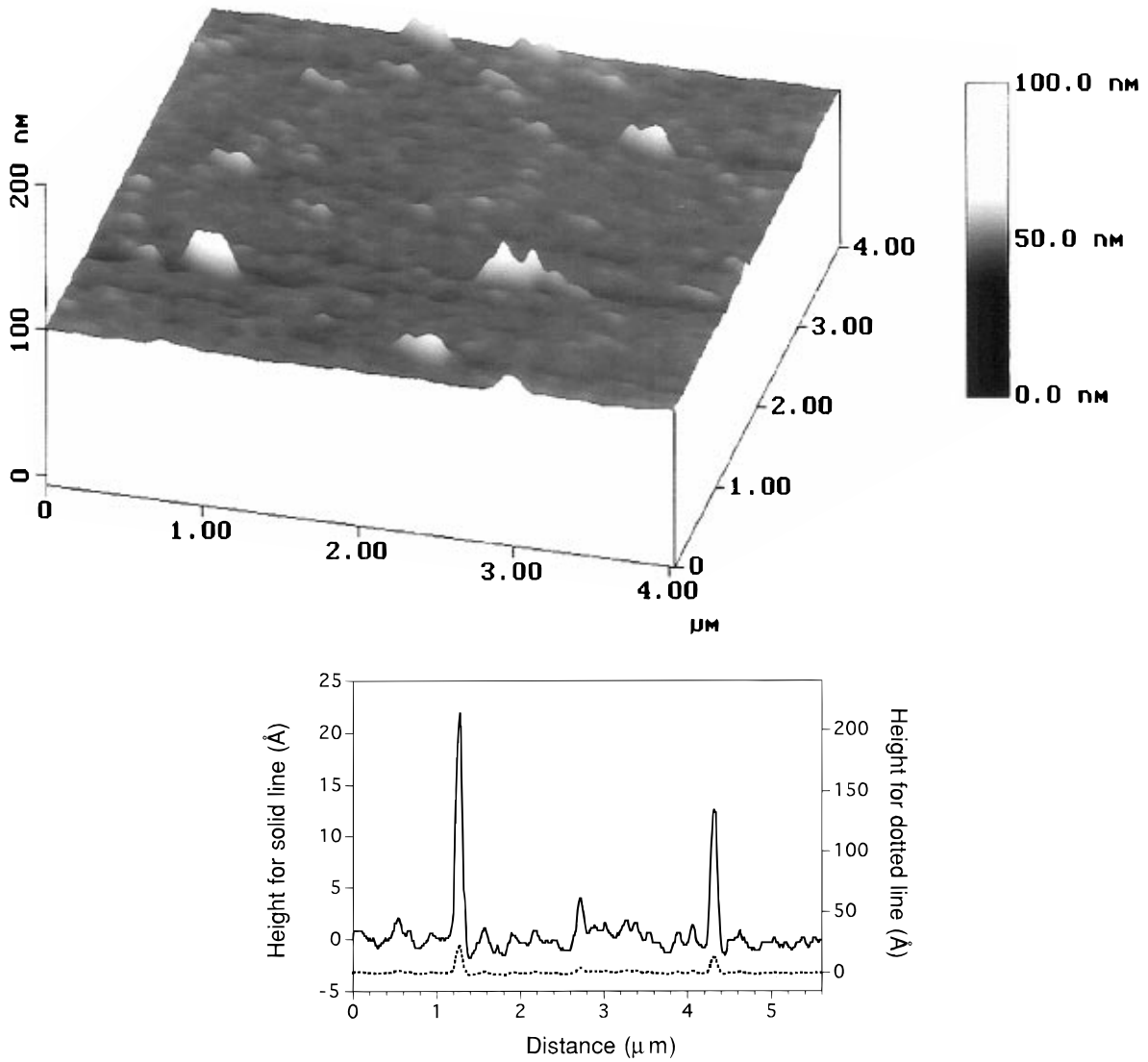

Figure 3. (top) AFM image of a 10 layer ZrPAPD film on Si. The rms roughness is 17 Å, and the *Z* range is 100 nm. (bottom) Line scan from the above image for a line drawn from the lower left-hand corner to the upper-right hand corner. The line related to the course scale (−50 to +200 Å) is for comparison to Figures 4 and 6.

phenylenediammonium), which would only require $^3/_4$ of a Zr^{4+} per formula unit. Thus, the expected ratio of Zr:P in ZrBAB is 0.75:2, as observed. The model typically used to describe the structure of these metal phosphonate films involves an α-ZrP inorganic sheet (Zr:P ratio of 1:2) with pendent organic groups. The most plausible structure for ZrBAB films has a close packed network of $-PO_3$ groups, with Zr^{4+} vacancies in the α-ZrP layer. Protonation of the phenylenediamine moiety makes it a much poorer donor than the neutral form. To increase donor strength, we are investigating other groups that will not form protonated species under our deposition conditions. It is important to note, however, that the protonated form of BAB does act as an efficient donor toward strong acceptors, such as viologen, in multilayer thin films.[32]

We have seen evidence previously for preorganization of α,ω-alkylbisphosphonic acids into lamellar structures in solution prior to deposition.[26] The driving force for this preorganization in solution is the van der Waals interaction between the long alkyl chains used in our study ($-(CH_2)_{16}-$). The singly protonated BAB molecule may also aggregate into lamellar structures in solution, due to both van der Waals and hydrogen-bonding interactions between phenylenediammonium groups. Forming lamellar structures in solution may be a key component in obtaining ordered, flat films of metal bisphosphonates.

We have previously described the preparation and photochemistry of zirconium *N*,*N*′-bis(2-phosphonoethyl)-4,4′-bipyridine dihalide (ZrPV(X), see Scheme 1) films and solids.[33,34] More recently, the structure of the solid was reported to be unlike that of existing zirconium phosphates or phosphonates.[35,36] The formula was determined to be $Zr_2(O_3PCH_2CH_2-viologen-CH_2CH_2-PO_3)X_6 \cdot H_2O$, corresponding to three halide ions per Zr atom. The halide ions in this structure are all coordinated to the Zr atoms, such that $(ZrX_3)_2$(bisphosphonate)$\cdot H_2O$ is a more accurate description. This formula

(32) Byrd, H.; Suponeva, E. O.; Bocarsly, A. B.; Thompson, M. E. *Nature*, submitted for publication.

(33) Vermeulen, L. A.; Snover, J. L.; Sapochak, L. S.; Thompson, M. E. *J. Am. Chem. Soc.* **1993**, *115*, 11767−11774.

(34) Vermeulen, L. A.; Thompson, M. E. *Nature* **1992**, *358*, 656.

(35) Poojary, D. M.; Reis, K.; Clearfield, A.; Thompson, M. E., results to be published.

(36) Poojary, D. M.; Vermeulen, L. A.; Vicenzi, E.; Clearfield, A.; Thompson, M. E. *Chem. Mater.* **1994**, *6*, 1845−1849.

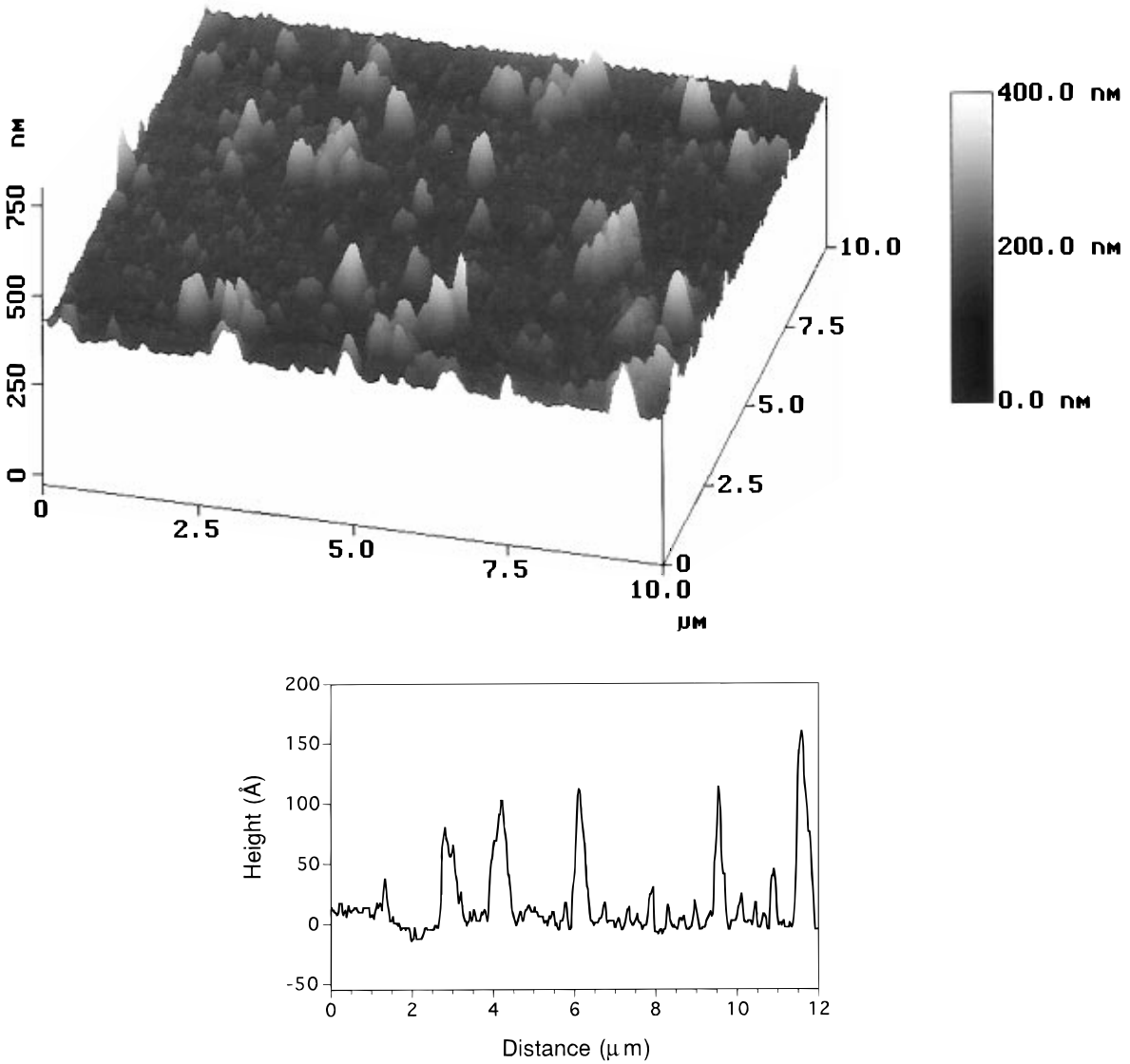

Figure 4. (top) AFM image of an eight-layer ZrPV(Cl) film on Si. The rms roughness is 220 Å, and the *Z* range is 400 nm. (bottom) Line scan from the above image for a line drawn from the lower right-hand corner to the upper left-hand corner.

gives a ratio of Zr:P = 1:1 instead of the expected value of 1:2 for a typical zirconium bisphosphonate compound.

Considering the novel structure observed for the microcrystalline solid, it is important to establish the structure of the thin films. We see very different behavior for films grown with viologen bisphosphonates, relative to alkyl bisphosphonate of BAB films. Films grown on fused SiO_2 substrates show a linear increase in absorbance, but they do not show uniform growth based on ellipsometric results on Si. The average of multiple measurements increases linearly, but with a very large deviation (±40 Å) in the data collected at different points on the substrate. AFM images of eight layers of ZrPV(Cl) on Si reveal large islands of material (Figure 4). The rms roughness of this surface is 220 Å, indicating that the film is not growing in a layer-by-layer manner but rather growing as discrete crystallites. The presence of these large features explains the spread in ellipsometric data. The nature of this film is decidedly nonlayered and is an example of a new class of metal phosphonate "film" growth.

The novel structure of the ZrPV(X) microcrystalline solids is proposed to result from electrostatic repulsion of adjacent viologen groups.[36] The observed structure increases the viologen^{2+}−viologen^{2+} distance, thereby reducing the electrostatic interactions. EPMA of microcrystalline samples of ZrPV(X) have the expected 1:1 ratio for Zr:P.[36] EPMA measurements on ZrPV(Cl) crystallite films show the Zr to P ratio is 1:1 in the films as well. Films grown with hafnium also showed a 1:1 metal (Hf) to P ratio. The fact that identical stoichiometries were observed for the solids and films suggests that similar structures are being adopted in both forms of ZrPV(X). The above data also suggest that the ZrPV(X) films are not growing layer by layer but rather are forming ZrPV(X) crystallites on the surface. The close similarities in photochemical processes reported for both thin films and microcrystalline samples of ZrPV(X)[36] are not surprising, since they appear to be the same materials.

If electrostatic interactions are responsible for the crystallite film growth of ZrPV(X), then an isostructural neutral species should grow flat with the conventional Zr to P ratio (1:2). Multilayers of zirconium 4,4′-bis(2-phosphonoethyl)biphenyl (ZrEPB, see Scheme 1) were prepared and analyzed to test this hypothesis. This bisphosphonic acid should be structurally identical to viologen bisphosphonic acid but contains an uncharged

Table 1. Metal-to-Phosphorous Ratio for Several Metal Viologen Phosphonates (Determined by Electron Probe Microanalysis)

film	ZrPV(Cl)	HfPV(Cl)	ZrPV(Br)	ZrPV(I)	ZrPV($PtBr_4^{2-}$)	ZrEPB
metal:P	1.0:1.1	1.0:1.0	1.0:1.5	1.0:2.5	1.0:1.8:1.3 (Pt)	1.0:2.0

organic group. The data for this film are indicative of an ordered, lamellar structure. UV/vis and ellipsometric plots for growing ZrEPB films are linear, with very little deviation in data collected at different points on the substrate. AFM images of 10 layers of ZrEPB on Si give an rms roughness of 25 Å and do not have any large islands of material. This roughness value indicates that while the surface of this film is not completely smooth, it is significantly different from that of the ZrPV(Cl) surface. The Zr:P ratio, as determined by microprobe analysis, gives the expected value of 1:2. The characterization of this lamellar film supports the notion that island formation in ZrPV(X) crystallite films is due not to the structure of the bisphosphonic acid but rather to the cationic charges of viologen.

The dicationic viologen requires halogen anions to balance charge. The sizes of the halogens are considerably different moving down the periodic table. If the size of the halogen anion affects the film structure, this would be reflected in the Zr:P ratio. Table 1 shows that the Zr:P ratio becomes richer in P on going from Cl to Br to I films. The values for a film that has $PtBr_4^{2-}$ exchanged for free halides is also included and falls very close to the conventional values expected for zirconium phosphonates, i.e., 1:2. All of these films showed very low halogen content when examined by EPMA. We suspect that the electron beam is in some way disturbing the halides (e.g., inducing desorption), since the halogen concentrations have been independently determined by titration methods for the bulk solids.[36] These data show that the identity of the counterion does influence the composition and thus the structure of the film. The value for the Br film is between that of ZrPV-(Cl) and the conventional [i.e., $Zr(O_3PR)_2$] ratio, suggesting that it could either be a mixture of two structure types or some intermediate structure giving rise to this composition. The I film is rich in viologen bisphosphonate, suggesting I is difficult to accommodate in the film lattice, leading to an alternate structure, which also leads to crytallite growth. AFM images of these films are not significantly different from one another.

We are interested in constructing composite multilayers consisting of adjacent layers with different photoactive materials. To study the growth of these mixed systems, a film of ZrPV(Cl) was grown on top of a film of ZrBAB. Figure 5 shows the increase of UV/vis absorption for 10 layers of ZrBAB followed by 10 layers of ZrPV(Cl). AFM images of these multilayers reveal a surface, which is smooth before the viologen film is initiated but forms the large islands associated with pure ZrPV(Cl) crstallite films after several layers are grown. Thus growing ZrPV(X) films on a flat metal phosphonate film does not alter its crystallite-like growth pattern.

Our original photophysical experiments indicated that the primary photoprocess in ZrPV(X) films regardless of the electron donor is the $\pi \rightarrow \pi^*$ absorption of the viologen.[33] This band is centered at 270 nm in the ultraviolet region of the spectrum. In an effort to shift this photochemistry to the visible region, we have

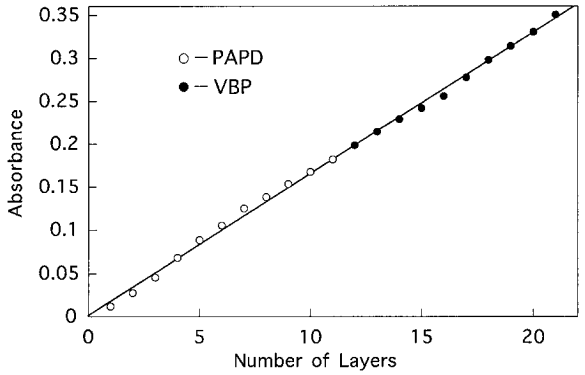

Figure 5. Absorbance as a function of layers for 10 layers of ZrPV(Cl) grown on 11 layers of ZrPAPD. Absorption was obtained on SiO_2 substrates at 270 nm.

prepared compatible molecules with lower energy absorptions. *N*,*N*′-Bis(2-phosphonoethyl)-4,4′-bis(4-vinylpyridine)biphenyl dichloride (VPB(Cl), see Scheme 1) has a broad absorption centered at 400 nm and is structurally similar to the viologen bisphosphonic acid. Films of ZrVPB(Cl) were prepared on Si and SiO_2 substrates and showed a similar crystallite growth pattern to that discussed for ZrPV(X) films. Microprobe analysis of a crystallite film of ZrVPB(Cl) gave a Zr:P ratio of 1:1, similar to the ZrPV(Cl) film. The surface of this film is also very similar to ZrPV(X) with large islands (rms roughness = 98 Å for a 10-layer film). These data are in agreement with electrostatic repulsions being the driving force for crystallite growth.

The charge of the viologen apparently disrupts the normal multilayer growth motif. If charges in the organic material can affect film growth so dramatically, we were curious as to whether charged species added to the growth solution could also alter film growth. To examine this, we chose to grow films of ZrBAB in the presence of ammonium ion. A 5 mM solution of BAB with 10 mM ammonium chloride was used to grow a 10-layer film of ZrBAB on Si. With the exception of the addition of the ammonium ion to the acid solution, the growth procedure was identical with that described in the Experimental Section. The pH of the acid solution is not affected by addition of ammonium ion. The AFM image of this surface shows a dramatic change in the nature of the film growth of ZrBAB upon adding the ammonium ion to the bisphosphonic acid solution (Figure 6). The 10-layer film produced has an rms roughness of 380 Å, compared to an rms roughness of 17 Å for the same material grown in the absence of ammonium ion. Similar results were observed for films of ZrEPB grown with added tetramethylammonium cation (10 layers of ZrEPB grown with and without added NMe_4^+ ion have rms values of 250 and 28 Å, respectively). ZrEPB films grown with and without tetramethylammonium ion were examined by EPMA and showed identical Zr:P ratios of 1:2, indicating that the added cations are not affecting the film composition. The reason ammonium ions induce crystallite formation is not known. One possible explanation may be that the ammonium ions disrupt the formation of lamellar

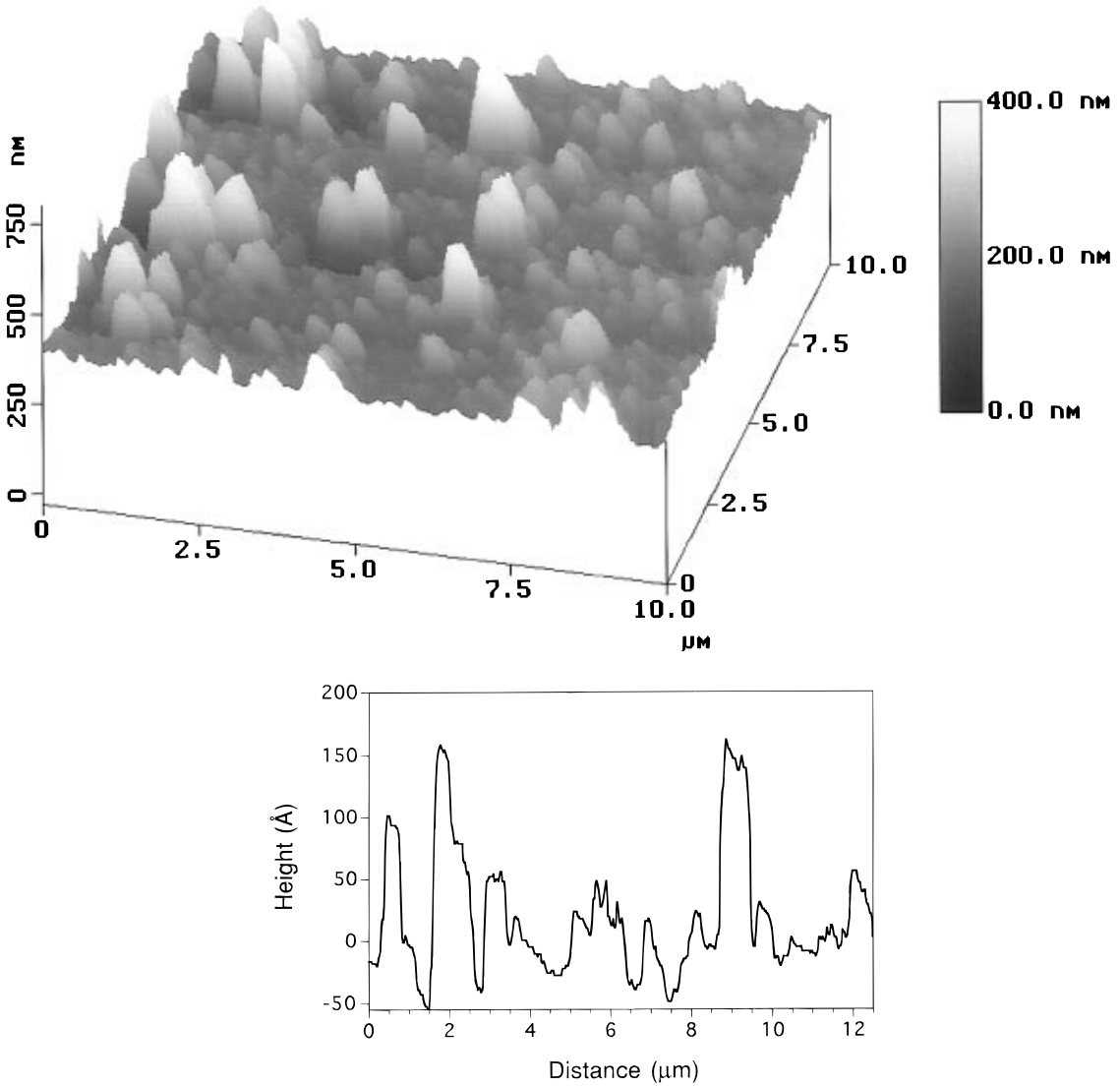

Figure 6. (top) AFM image of a 10-layer ZrPAPD film on Si grown with added ammonium chloride in the bisphosphonic acid solution. The rms roughness is 380 Å, and the *Z* range is 400 nm. (bottom) Line scan from the above image for a line drawn from the lower right-hand corner to the upper left-hand corner.

aggregates of the bisphosphonic acids in solution, which may be an important preassembly process for formation of uniform films.[26] Another possible explanation for the action of ammonium ions is that they temporarily substitute for Zr cations in the film, promoting Ostwald ripening to a crystallite film rather than the lamellar form.

We are investigating the effects that other added ions have on the growth of ZrBAB and ZrPV(X) films as well as other metal bisphosphonate films, in the hope that we can find a suitable ionic template to promote the growth of uniform films from bisphosphonic acids with charged organic groups. In addition to ionic templates, we are investigating the effect that neutral templates and different solvent mixtures have on the nature of metal phosphonate film growth.

Electrochemistry of ZrPV(X) on Gold Electrodes. Viologen bisphosphonate halides (Br and Cl) show a reversible one-electron reduction with $E° \sim -0.67$ V (SCE) at both GCE and Au electrodes in aqueous solutions (Figure 7A). This is close to the $E°$ of methylviologen dication one-electron reduction (−0.68 V).[37] The reduction of the viologen moiety in ZrPV(X) crystallite films proceeds at more negative potentials (Figure 7B; Figure 8, insert). The reduction product is viologen cation radical as shown by spectroelectrochemical measurements for films of ZrPV(Cl) grown on Sn[Sb]O_x-coated glass substrates (Figure 8). Both viologen cation monomers with absorption maxima at 400 and 600 nm (as compared to 399 and 610 nm in solution)[38] and dimers with absorption maxima at 375 and 560 nm (as compared to 380 and 540 nm in solution)[39] are formed during electrolysis of the crystallite films. The monomer is the prevalent viologen reduction product in photolyzed ZrPV(Cl) films,[33] suggesting that electrolysis leads to more thorough reduction of this crystallite film than photolysis.

As shown in Figure 9, the cathodic charge passing through ZrPV(X) films grown on gold substrates in the course of their reduction increases with the film thickness (i.e., number of depositions or cycles in Figure 1). It is difficult to say if the increase is linear because the peaks are poorly defined, especially for very thin films where the charge estimates are less precise. The

(37) Bird, C. L.; Kuhn, A. T. *Chem. Soc. Rev.* **1981**, *10*, 49−82.
(38) Feng, Q.; Yue, W.; Cotton, T. M. *J. Phys. Chem.* **1990**, *94*, 2082−2091.
(39) Kosower, E. M.; Cotter, Y. L. *J. Am. Chem. Soc.* **1964**, *86*, 5524.

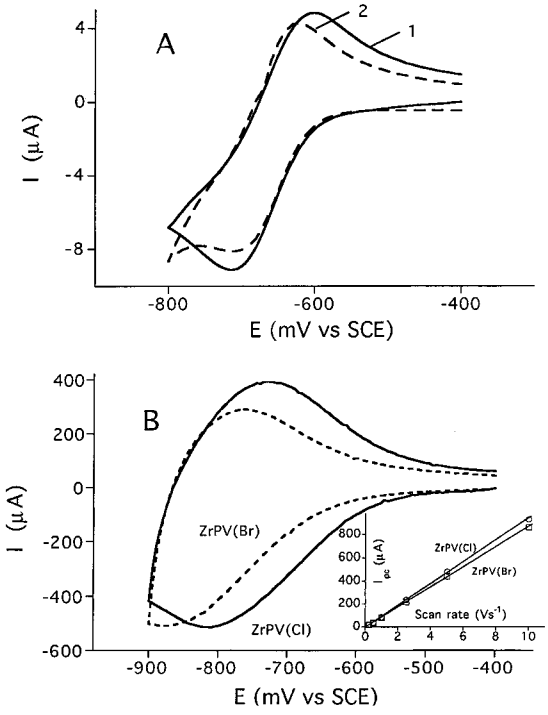

Figure 7. (a) Cyclic voltammograms of 10^{-3} M PV(Cl) in 0.1 M $NaClO_4$ (aq) on GCE (1) and 0.1 M Na_2SO_4(aq) on Au (2). Scan rates: 0.1 V s^{-1} (1) and 0.25 V s^{-1} (2). (b) Cyclic voltammograms of thin films (four depositions) of ZrPV(Cl) in 0.1 M KCl(aq) (solid lines) and ZrPV(Br) in 0.1 M KBr(aq) (dashed lines) on Au electrode (surface area 0.22 cm^2) at the potential scan rate 5 V s^{-1}. Insert represents the dependence of the cathodic peak current on the potential scan rate.

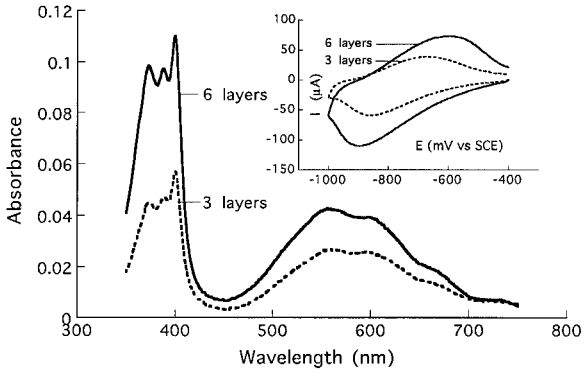

Figure 8. Absorption spectra of viologen cation radical produced in the ZrPV(Cl) films on Sn[Sb]O_x optically transparent electrodes by 2 min electrolysis at −0.9 V vs SCE. The cyclic voltammograms of these films in 0.1 M KCl(aq) before electrolysis are shown in the insert (scan rate 0.25 V s^{-1}).

cathodic peak current shows linear dependence on the scan rate (Figure 7B, insert) characteristic of the nondiffusional surface process.[40] The shape of the peaks (Figure 7B) and the significant cathodic-anodic peak separation, even for very thin films(Figure 10), are not typical for surface waves and indicate that some kinetic limitations for electron transfer in the crystallite films exist. On the basis of the structural data available about these materials,[35,36] the counteranion for the viologen groups in the crystallites are negatively charged Zr centers (i.e., $(ZrX_3R_3)^-$ centers, X = halide, R = phosphonate oxygen, two of which are −1 and one is neutral). On reduction of the viologen group, the counteranion should leave the structure, which can happen only by hydrolysis of one of the zirconium-bound halide ions, with associated changes in the film structure. It was reported previously that a number of structural rearrangements are involved in the photochemical formation of charge-separated states in these materials.[33] This chemical step, with the consequent structural rearrangements, results in a certain stabilization of the reduced product that manifests itself in a shift of the anodic peak corresponding to the product

(40) Murray, R. W. *Introduction to the Chemistry of Moleculary Designed Electrode Surfaces*; Murray, R. W., Ed.; John Wiley & Sons, Inc.: New York, 1992; Vol. 22, pp 1−48.

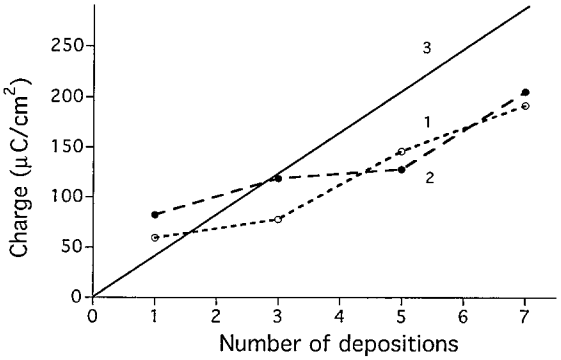

Figure 9. Cathodic charges passed through Au electrode in the course of electrochemical reduction of ZrPV(Cl) films in aqueous 0.1 M KCl solutions (1) and of ZrPV(Br) films in aqueous 0.1 M KBr solutions (2). Curve 3 represents the theoretically expected amount of charge vs number of depositions in the assumption that every deposition results in a monolayer coating with 39 Å^2 per viologen and all viologens undergo one-electron reduction.

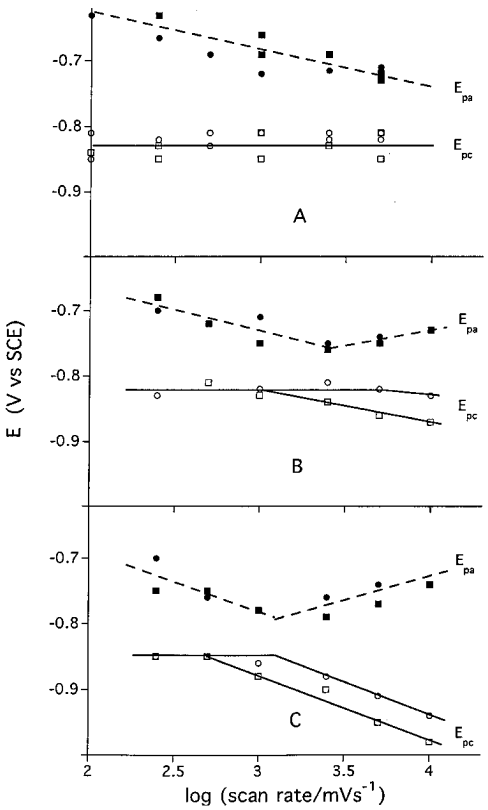

Figure 10. Positions of the cathodic and anodic peak potentials (E_{pc} and E_{pa}, respectively) on cyclic voltammograms of ZrPV(Cl) (circles) and ZrPV(Br) (squares) registered at different potential scan rates. Film thickness: (A) 1−3 depositions; (B) 5 depositions; (C) 7 depositions.

reoxidation to more positive potentials. This effect is more pronounced when the time scale is increased (at lower potential scan rates, Figure 10). The structural reorganization may be faster in thin crystallite films (i.e., smaller or less ordered crystallites) and is most likely the reason thin films show larger cathodic−anodic peak separation than thicker films at the low scan rates.

The cathodic peak potentials (E_{pc}'s) are practically constant at all potential scan rates studied (up to 10 V s^{-1}) for thin crystallite films (Figure 10A), so the direct electron-transfer step should be very fast in these materials. For thicker crystallite films the dependence of the E_{pc} on the log(scan rate) shows a shift to more negative potentials, which starts earlier when the film thickness increases (Figure 10B,C). The shift of the E_{pc} to more negative potentials is accompanied by a shift of the anodic peak potentials ($E_{pa's}$) to more positive values, indicating kinetic limitations for both cathodic and anodic processes. It is interesting that the films composed of ZrPV(Cl) and ZrPV(Br) show some differences in the electrochemical behavior: The deviation of the E_{pc} from the straight line starts at higher potential scan rates for ZrPV(Cl) than for ZrPV(Br), which may be related to the differences in the growth patterns of these films. On the basis of the electrochemical data shown, the charge propagation through the ZrPV(Cl) film is more facile than a ZrPV(Br) film.

For the thin crystallite films of ZrPV(X) it is possible to estimate the $E°_{surf}$ for the viologen dication/radical cation couple by extrapolating the E_{pa} and E_{pc} lines (Figure 10A) to higher scan rates to find their intersection. The $E°_{surf}$ value estimated in this way is about −0.83 V. The E_{pc} and E_{pa} values for thicker films show a more complex dependence on the scan rate. They appear to converge with the increasing scan rate for the scan rates between 0.1 and ∼2 V s^{-1}, which suggests that as the time scale is decreased structural rearrangement in the crystallites is less important (as observed for thin films). Then, at higher scan rates, E_{pc} and E_{pa} diverge, indicating that the rate of viologen reduction becomes limited by charge propagation through the film. This effect is more pronounced with thicker films. In this case $E°$ may be calculated in a way used for a diffusion-limited process: as $E° = (E_{pc} + E_{pa})/2$, and it is close to −0.83 V again (ZrPV(Cl) = −0.83 V and ZrPV-(Br) = −0.85 V).

Thus, $E°$ of viologen groups in ZrPV(X) crystallite films is independent of the film thickness in the thickness range corresponding to 1−7 depositions. The reduction of viologen groups in these films proceeds at potentials at least 150 mV more negative than those reported in the literature reduction of viologen derivatives in solutions[37] and films.[41−44] This means that the viologen radical cation generated electro- or photochemically in ZrPV(X) films has higher reducing power, which makes this system very attractive for such applications as H_2 production from water.

Experimental Section

UV/vis absorption spectra of films on transparent substrates were recorded on a computer-interfaced Cary 14 Model 14 DS spectrometer. Ellipsometric thicknesses of films grown on silicon substrates were measured using a Gaertner L116D ellipsometer equipped with a HeNe laser. AFM images were obtained using a Nanoscope III Multimode microscope in the tapping mode. Proton NMR spectra were obtained on a GE QE-300 spectrometer. Cyclic voltammograms (CV) were registered at Au electrodes (typical working surface area 0.2−0.3 cm^2) covered with ZrPV(X) films as described below using a PAR Model 283 potentiostat/galvanostat. The counter electrode (Pt wire) was separated from the working solution by a porous glass frit. The supporting electrolytes were usually 0.1 M KCl aqueous solution for ZrPV(Cl) films and 0.1 M KBr aqueous solution for ZrPV(Br) films. The reference was a saturated calomel electrode (SCE). Oxygen was removed from the working solution by bubbling with argon gas of high purity.

Deionized water was obtained from a Barnstead Nanopure II. All commercial reagents (Aldrich) and solvents were used as received unless otherwise stated.

Electron Probe Microanalysis. Electron probe microanalysis (EPMA) was performed on a CAMECA SX-50 at the Princeton Materials Institute's Electron Microbeam Facility. Conditions for collecting X-ray microanalytical data included an accelerating voltage of 15 kV, a regulated beam current of 20 nA, and a defocused electron probe 10 μm in diameter. Multiaccelerating voltage (5, 10, and 15 kV) measurements were performed on a single metal phosphonate film in order to remove the effects of exciting substrate material (see characterization results above). The following reference compounds and minerals were used as calibration standards: ZrO_2 (Zr Lα), $Ca_5(PO4)_3F$ (P Kα), Al_2O_3 (O Kα), Pt (Pt Mα), Hf (Hf Lα), SnO_2 (Sn Lα), Kbr (Br Lα), LaB_6 (La Lα), Ni (Ni Kα), Zn_2SiO_4 (Zn Kα), along with Si or $CaSiO_3$ (Si Kα) depending upon the substrate composition. Matrix corrections were performed using the $\Phi(\rho,Z)$ method.

Syntheses: *Synthesis of 1,4-Bis(4-phosphonobutylamino)-benzene (BAB).* ($H_2O_3P-(CH_2)_4-NHC_6H_4NH-(CH_2)_4-PO_3H_2$). *p*-Phenylendiamine (5.0 g, 0.046 mol) and diethyl (4-bromobutyl)phosphonate (15.6 g, 0.114) were refluxed in 50 mL of THF in the presence of 1.56 g of NaH for 2 days. After cooling, 50 mL of H_2O was slowly added to the reaction mixture. The solution was extracted three times with 100 mL portions of $CHCl_3$. TLC showed the desired product was in the $CHCl_3$ layer. Decolorizing charcoal was added to the $CHCl_3$ solution and stirred for 1 h and then filtered. The $CHCl_3$ solution was taken to dryness, leaving a brown oil. ^1H NMR (D_2O), 6.9 (4H, s), 3.1 (4H, triplet), 1.5 (12H, multiplet) ppm. Mass spectrum: E.I., M^+(obs) = 492, M^+(theor) = 492; major fragments: 446, 354, 193, 137, 125. The ester was hydrolyzed to the acid by refluxing in 6 M HCl for 2 days. The acid was precipitated from this solution by the addition of acetone. Overall yield 10%.

Synthesis of Viologen Bisphosphonic Acid Salts [N,N′-Bis-(2-phosphonoethyl)-4,4′-bipyridine dihalide] (PV(X)). ($H_2O_3P-(CH_2)_2$-4,4′-bipyridinium$-(CH_2)_2-PO_3H_2$). The viologen dichloride salt was prepared by reacting 1.2 g (6.0 mmol) of diethyl (2-chloroethyl)phosphonate with 0.47 g (3.0 mmol) of 4,4′-bipyridine in 120 mL of H_2O at 110 °C for 40 h. The ester was converted to the acid by refluxing in 6 M HCl. The viologen dibromide salt was prepared as above except diethyl (2-bromoethyl)phosphonate was used. The ester was dried under vacuum and then converted to the acid by overnight stirring with a 3-fold excess of bromotrimethylsilane in dry acetonitrile followed by the addition of water. The viologen diiodide salt was prepared by adding $AgPF_6$ to a solution of the viologen dichloride salt to precipitate AgCl. When the viologen dihexafluorophosphate salt was isolated, an excess of KI was added to the solution. The resulting reddish-brown solid was isolated by filtration. All viologen salts were purified by dissolving in a minimum volume of water and precipitated by the slow addition of isopropyl alcohol. ^1H NMR of all salts (D_2O) 9.1 (4H, doublet), 8.5 (4H, doublet), 4.2 (4H, multiplet), 2.0 (4H, multiplet) ppm. CHN analysis of $H_2O_3P-(CH_2)_2$-4,4′-bipyridinium$-(CH_2)_2-PO_3H_2Br_2$: theoretical, C 31.47, H 3.77, N 5.24; found, C 32.38, H 4.39, N 5.82.

Synthesis of 4,4′-Bis(2-phosphonoethyl)biphenyl (EPB). ($H_2O_3P-(CH_2)_2-$(4,4′-biphenyl)$-(CH_2)_2-PO_3H_2$). In a dry glass

(41) De Long, H. C.; Buttry, D. A. *Langmuir* **1992**, *8*, 2491−2496.
(42) Huang, J.; Wrighton, M. S. *Langmuir* **1993**, *9*, 3291−3297.
(43) Lee, C.-W.; Bard, A. J. *Chem. Phys. Lett.* **1990**, *170*, 57−60.
(44) Katz, E.; de Lacey, A. L.; Fierro, J. L. G.; Palacios, J. M.; Fernandez, V. M. *J. Electroanal. Chem.* **1993**, *358*, 247−259.

pressure tube, 3.8 g (9.4 mmol) of diiodobiphenyl, 3.23 g (20 mmol) of diethyl vinylphosphonate, 0.05 g (0.2 mmol) of palladium acetate, and 0.23 g (0.7 mmol) of tritolylphosphine were dissolved in 20 mL of dry triethylamine and 30 mL of dry toluene. The mixture was purged with Ar for 10 min and then closed. The reaction was heated to 110 °C with stirring for 24 h. Approximate yield of 4,4′-bis(diethyl vinylphosphonate)biphenyl was 30%. ^{1}H NMR (DMSO) 7.8 (8H, multiplet), 7.4 (2H, doublet), 6.5 (2H, triplet), 4.0 (8H, multiplet), 1.2 (12H, triplet) ppm. Mass spectrum: E.I., M^+(obs) = 478, M^+(theo) = 478; major fragments: 369, 341, 313, 231, 202. This intermediate was hydrogenated with Pd/C in methanol to give an oil. To the ester were added 20 mL of dry CH_2Cl_2 and 1 mL of bromotrimethylsilane. After the addition of water and separation with ether, the acid was isolated. ^{1}H NMR ($CDCl_3$) 7.4 (8H, doublet), 2.9 (4H, multiplet), 2.1 (4H, multiplet) ppm. Overall yield ca. 20%.

Synthesis of N,N′-Bis(2-phosphonoethyl)-4,4′-bis(4-vinylpyridine)biphenyl Dichloride (VPB) ($H_2O_3P(CH_2)_2NC_5H_4CH$═CH-(4,4′-biphenyl)CH═$CHNC_5H_4(CH_2)_2PO_3H_2$). In a dry glass pressure tube, 1.04 g (2.6 mmol) of diiodobiphenyl, 3.0 mL (27 mmol) of vinylpyridine, 0.09 g (0.36 mmol) of palladium acetate, and 0.2 g (0.6 mmol) of tritolylphosphine were dissolved in 8 mL of dry triethylamine and 20 mL of dry acetonitrile. The mixture was purged with Ar for 15 min and then closed. Reaction was heated to 110 °C with stirring for 48 h. Approximate yield of 4,4′-bis(4-vinylpyridine)biphenyl was 30%. ^{1}H NMR ($CDCl_3$) 8.9 (4H, doublet), 8.2 (4H, doublet), 8.1 (4H, doublet), 7.9 (4H, doublet), 7.6 (4H, doublet) ppm. Mass spectrum: E.I., M^+(obs) = 360, M^+(theo) = 360; major fragments: 266, 180, 91. 0.3 g (0.83 mmol) of this was combined with 0.5 g (2.0 mmol) of diethyl 2-bromoethylphosphonate in a round-bottom flask and dissolved in 10 mL of DMF. Mixture was heated at 90 °C for 16 h until a yellow precipitate was observed. DMF was vacuum distilled, and the yellow ester was obtained. To the ester were added 10 mL of dry CH_2Cl_2 and 1 mL of bromotrimethylsilane. The mixture was stirred for 12 h, and then H_2O was added causing an orange precipitate. Solid was isolated and recrystallized from H_2O by the slow addition of cold methanol. NMR showed the disappearance of the ester peaks indicating the acid was formed. ^{1}H NMR (DMSO) 8.42 (4H, doublet), 8.22 (4H, doublet), 7.55 (8H, multiplet), 7.04 (4H, doublet), 4.26 (4H, triplet), 1.41 (4H, triplet) ppm.

Film Deposition. Fused silica and single-crystal silicon substrates were cleaned in a 1:3 solution of 30% H_2O_2 and concentrated H_2SO_4 (**caution**: mixture reacts violently with organics). Substrates were rinsed thoroughly with deionized water then dried in an oven at 150 °C for 30 min. Substrates were silated by suspending them above a refluxing solution of 3% triethoxy(3-aminopropyl)silane (Petrarch) in toluene in a nitrogen atmosphere for 16 h.[45] Phosphonation of the amine-terminated surface was accomplished by treating with a 4% solution of $POCL_3$ and 2,6-lutidine in dry acetonitrile.[16] After rinsing with water, the substrates were ready for treatment in metal solution.

ZrPV(X), HfPV(Cl), and ZrVPB films were grown by alternate treatment in 5 mM bisphosphonic acid solution at 50 °C for 4 h and room-temperature treatment in 20 mM $ZrOCl_2$ for 2 h. Films of ZrBAB were grown by alternate treatment in 5 mM BAB solution (aq) for 3 h at room temperature and 20 mM $ZrOCl_2$ for 2 h. Films of ZrBAB were also grown using the same technique with the addition of 2 equiv of ammonium chloride.

Gold foil (0.05−0.1 mm thick) and optically transparent $SnSbO_x$-coated glass slides (Delta Technologies; 100 Ω/square) were used as substrates for growth of ZrPV(X) films for electrochemical measurements. Au foil was initialized with (4-mercaptobutyl)phosphonic acid[46] (10 mM solution in ethanol) overnight to produce a phosphonic acid rich surface. $SnSbO_x$ substrate was silanized in 2% solution of (3-aminopropyl)dimethylethoxysilane (Gelest) in toluene overnight, then amino groups were phosphonated by treatment in acetonitrile solution of $POCl_3$ and 2,4-lutidine (10 mM of each) for 10 h at room temperature. The films were deposited by repeated dipping of the substrate in 60 mM $ZrOCl_2$ aqueous solutions for 2 h at room temperature and then in 10 mM aqueous viologen solutions for 4 h at 80 °C. The surface was thoroughly rinsed with distilled water between dippings.

Conclusion

We have presented data which show that zirconium bisphosphonic acid thin films can be grown as either uniform lamellar films or crystallites on a planar substrate. Our initial intent in producing thin films with phenylenediamine groups in the bisphosphonate molecule was to use these films as potent electron donors in multilayer assemblies. Under growth conditions, however, a protonated species is formed, which should significantly decrease its donor strength. We are currently investigating other donor substituted bisphosphonates, which will not be protonated under the growth conditions. Bisphosphonic acids which typically form uniform multilayers can be induced to grow films in a highly nonuniform, crystallite manner by adding ammonium ions to the bisphosphonic acid growth solution. We are currently investigating the effects that added ions or templating agents have on the growth of metal bisphosphonate thin films, in order to determine the appropriate growth conditions to form well ordered, uniform films from bisphosphonic acids containing cationic organic groups.

The composition and photochemistry of ZrPV(X) films is affected by the chosen halide. EPMA data show the Zr to P ratio increases as the size of the halide increases. Macroscopic electron transfer was investigated by studying the electrochemical properties of ZrPV(X) films (on Au electrodes). The reduction potential of viologen is 150 mV more negative than that of viologen species in solution. This means that the viologen radical cation generated electro- or photochemically in ZrPV(X) films has higher reducing power than the viologen radical cation in solution, which makes this system very attractive for photocatalytic reductions, such as H_2 production from water.

Acknowledgment. The authors gratefully acknowledge the American Biomimetics Corp. and the National Science Foundation (Grant CHE-9312856) for financial support for this work.

CM9600586

(45) Haller, I. *J. Am. Chem. Soc.* **1978**, *100*, 8050−8055.

(46) Hong, H.; Mallouk, T. E. *Langmuir* **1991**, *7*, 2362−2369.